Nanoscale

Accepted Manuscript

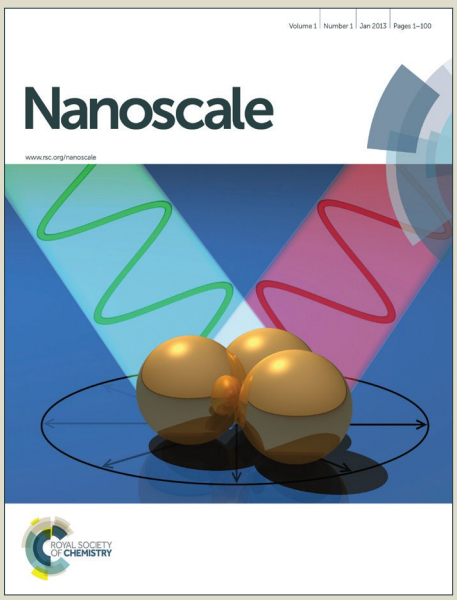

ROYAL SOCIETY OF CHEMISTRY

www.rsc.org/nanoscale

Nanoscale

PAPER

Fluorescent Graphitic Carbon Nitride Nanosheet Biosensor for Highly Sensitive, Label-Free Detection of Alkaline Phosphatase

Received 00th January 20xx,
Accepted 00th January 20xx

DOI: 10.1039/x0xx00000x

www.rsc.org/

Mei-Hao Xiang, Jin-Wen Liu, Na Li, Hao Tang*, Ru-Qin Yu and Jian-Hui Jiang*

Graphitic C_3N_4 ($g\text{-}C_3N_4$) nanosheets provide an attractive option for bioprobes and bioimaging application. Ultizing highly fluorescent and water-dispersible ultrathin $g\text{-}C_3N_4$ nanosheets, a highly sensitive, selective and label-free biosensor has been developed for ALP detection for the first time. The developed approach utilizes a natural substrate of ALP in biological systems, and thus affords very high catalytic efficiency. This novel biosensor is demonstrated to enable quantitative analysis of ALP in a wide range from 0.1 to 1000 U/L with a low detection limit of 0.08 U/L, which is among the most sensitive assays for ALP. It is expected that the developed method may provide a low-cost, convenient, rapid and highly sensitive platform for ALP-based clinical diagnostics and biomedical applications.

Introduction

Since the discovery of graphene, ultrathin two-dimensional (2D) atomic-thick nanosheets have attracted great attention for various applications including optical and electronic devices as well as biomedical probes.[1,2] Graphene and its derivatives have been shown to have many unique properties such as very high electron mobility, very high thermal conductivity, high fluorescence quenching efficiency and selective adsorption of single-stranded DNA over DNA of other conformations,[3-7] which makes them extremely popular in biosensing and bioprobe fields.[8-11] Other 2D transition metal nanomaterials such as $Bi_2Sr_2CaCu_2O_x$, WS_2, MoS_2 and $NbSe_2$ have also been demonstrated for bioanalysis and diagnostics.[12,13] However, these 2D nanomaterials are usually non-fluorescent or show relatively low fluorescence quantum yields, which limits their potential for biological analysis and imaging.[14,15] Moreover, heavy-metal containing 2D materials with perceptive toxicity may hamper their implementation in biological systems.[16] Therefore, the pursuit for 2D nanomaterials with strong fluorescence, high biocompatibility and low toxicity is highly demanded.

Graphitic C_3N_4 ($g\text{-}C_3N_4$) nanosheets provide an attractive option for bioprobes and bioimaging applications.[17-19] The $g\text{-}C_3N_4$ nanosheets are heavy-metal free and can be prepared to give high fluorescence quantum yield, high biocompatibility and low toxicity. Like graphene or its derivatives, this material is also demonstrated to adsorb selectively single-stranded DNA.[20,21] Moreover, the N-contain structure for the $g\text{-}C_3N_4$ nanosheet affords the ability for coordination with proton or metal ions.[22,23] These properties makes $g\text{-}C_3N_4$ nanosheets very useful for development of sensitive and label-free fluorescent biosensors or bioprobes. Utilizing the interactions between $g\text{-}C_3N_4$ nanosheet and metal ion or DNA molecule, several fluorescent biosensors or bioprobes have been developed for varying targets including nucleic acids,[20,21] copper and CN^- ions,[24] and organic molecules such as explosives and biothiols.[25-27] Nevertheless, the potential of $g\text{-}C_3N_4$ nanosheet for enzymatic sensor development has rarely explored.

Herein, we have developed a novel fluorescent $g\text{-}C_3N_4$ nanosheet based biosensor for highly sensitive, label-free detection of alkaline phosphatase (ALP). The development of convenient and reliable methods for monitoring ALP activity is valuable because ALP plays crucial roles in many biological processes and is a potential biomarker in clinical diagnosis.[28, 29] It is also an important label for immoassays and histochemistry.[30, 31] This assay is based on a recent finding that the strong fluorescence of $g\text{-}C_3N_4$ is able to be effectively quenched by copper ion via photoinduced electron transfer (PET).[22, 32] Because of the high affinity chelation between pyrophosphate (PPi) and Cu^{2+},[33-35] we hypothesize that the interaction between Cu^{2+} and pyrophosphate (PPi) may inhibit the coordination of $g\text{-}C_3N_4$ with Cu^{2+}. Motivated this hypothesis, we are able to develop a label-free sensor of ALP with the use of pyrophosphate (PPi) as its substrate.

Scheme 1 outlines the design principle for the proposed biosensor. The biosensor relies on the high affinity interaction between PPi and Cu^{2+}, which prevents coordination between $g\text{-}C_3N_4$ nanosheet and Cu^{2+}. In the absence of PPi, Cu^{2+} coordinates with the $g\text{-}C_3N_4$ nanosheets and quenches their fluorescence due to PET.[32]

State Key Laboratory of Chemo/Bio-Sensing and Chemometrics,
College of Chemistry and Chemical Engineering, Hunan University, Changsha, 410082, P. R. China. *E-mail:haotang@hnu.edu.cn; jianhuijiang@hnu.edu.cn;*
Tel: 86-731-88821916; Fax :86-731-88821916†
Electronic Supplementary Information (ESI) available. See DOI: 10.1039/b000000x

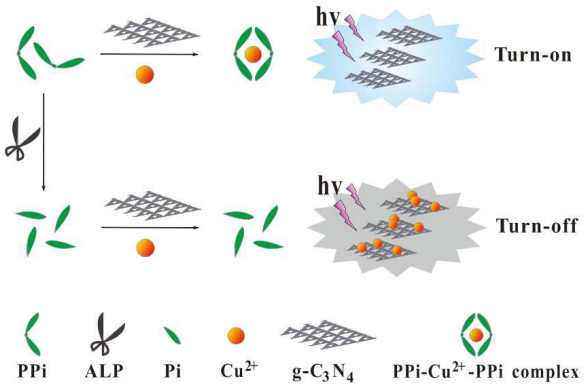

Scheme 1 Schematic representation of the label–free fluorescence assay for ALP detection utilizing fluorescent g-C_3N_4 nanosheets.

With the addition of PPi, Cu^{2+} forms a chelate with PPi,[33-35] which is unable to bind to the g-C_3N_4 nanosheets, resulting in a recovery of the fluorescence of the g-C_3N_4 nanosheets. In the presence of ALP, PPi is catalyzed to be transformed into phosphate (Pi) with much weaker interaction with Cu^{2+}, which releases Cu^{2+} from the Cu^{2+}/PPi complex and restores the coordination between Cu^{2+} and the g-C_3N_4 nanosheet. The quenched fluorescence, which is ascribed to Cu^{2+} released from its chelates with PPi, thus give an indicator for the activity of ALP. To our knowledge, this is the first time that g-C_3N_4 nanosheet has been exploited for the detection of ALP. Compared to existing methods for ALP assay typically involving the use of synthetic substrates,[36, 37] the developed approach utilizes a natural substrate of ALP in biological systems, which may afford higher catalytic efficiency toward this substrate and thus provide much better sensitivity for ALP detection. Relative to recently reported assays for ALP based on noble metal nanoclusters,[38, 39] g-C_3N_4 shows higher luminescent intensity as well as photo and chemical stability, which may ensure improved sensitivity and selectivity for the developed approach in ALP detection.

Experimental procedures

Materials and instruments

Alkaline phosphatase (ALP) was purchased from Thermo Fisher Scientific Inc., glucose oxidase (GOx), acetylcholinesterase (AChE), lysozyme, uricase were bought from Sigma-Aldrich., exo Ⅰ, exo Ⅲ exonuclease was purchased from New England Biolabs (Beijing), Ltd. Sodium pyrophosphate (PPi), potassium phosphate monobasic (KH_2PO_4), cupric sulfate ($CuSO_4$), magnesium chloride ($MgCl_2$), 2-[4-(2-Hydroxyethyl)-1-piperazinyl]ethanesulfonicacid (HEPES), were purchased from Sinopharm Chemical Reagent Co., Ltd. (Shanghai, China). Human serum was provided by Third Xiangya Hospital (Changsha, China). All chemicals used in this work were of analytical grade and directly used without additional purification. Ultrapure water (18.3 MΩ) which was obtained through a Millipore Milli-Q water purification system (Billerica, MA, USA) was used in the experiments.

The fluorescence measurements were carried out on a FL-7000 spectrometer (Hitachi, Japan). The fluorescence emission spectra of g-C_3N_4 were collected from 375 nm to 600 nm at room temperature with a 310 nm excitation wavelength. The fluorescence lifetime measurements were performed on a Fluorolog-Tau-3 spectrofluorometer (Jobin Yvon Inc., NJ). The transmission electron microscope (TEM) images were obtained on a field-emission high-resolution 2100F TEM (JEOL, Japan) at an acceleration voltage of 200 kV. The atomic force microscopy (AFM) image was performed by means of Bruker Bioscope system (Bruker, USA). X-ray diffraction (XRD) patterns of g-C3N4 samples were collected via a D8 Advance X-ray diffractometer (Bruker, USA)with Cu- Ka radiation (λ = 1.5418 Å).The infrared absorption spectroscopic measurements were taken with g-C3N4 powders in KBr pieces on a Nexus 870 FT-IR spectrophotometer (Thermo Electron, USA) under continuous N_2 purge. Dynamic light scattering (DLS) measurements were conducted using a Malvern Zetasizer 3000 HS particle size analyzer (Malvern Instruments, UK) in air at room temperature.

Synthesis of g-C_3N_4 nanosheets.

Bulk g-C_3N_4 material was fabricated from cyanamide according to previous report method.[40] Highly water-dispersible g-C_3N_4 nanosheets were prepared by chemically oxidizing with nitric acid and a liquid exfoliating method with minor modification.[41,42] Briefly, 2.0 g of bulk g-C_3N_4 powder was refluxed in 150 mL 10 mol·L^{-1} HNO_3 for 24 h. After cooling to room temperature, the refluxed product was centrifuged at 14, 000 rpm and washed with Mill-Q water until its pH reached 7. Then the refluxed product was dispersed in 50 mL water and ultrasounded consecutively for 20 h. The residual unexfoliated g-C_3N_4 was removed by centrifuging at 5000 rpm before use.

Fluorescence ALP assay

1 μL(ALP or other proteins) sample solutions with different final concentrations were added into 10 μL 1.2 mM PPi and 79 μL 10 mM HEPES (pH 7.4, 5 mM $MgCl_2$) at 37℃ for 30 min. Then 10 μL as-prepared g-C_3N_4 nanosheets and 20 μL 120 μM Cu^{2+} were added into the mixture to give a final volume of 120 μL at 37℃ for another 30 min. (final concentration of g-C_3N_4 nanosheets was 5 μg mL^{-1} and final concentration of Cu^{2+} was 20 μM).

For ALP detection in complex biological media, 1 μL ALP samples solutions with different final concentrations were added into 10 μL 1.2 mM PPi and 79 μL 10 mM HEPES (pH 7.4, 5 mM $MgCl_2$) containing 1% human serum at 37℃ for 30 min. The followed procedure was the same as shown in the aforementioned experiment for ALP detection in clean HEPES buffer.

ALP inhibitor evaluation

To study the inhibition of KH_2PO_4 on ALP activity, KH_2PO_4 solutions with different final concentrations were added into mixture of ALP (final concentrations of 2000 U/L), PPi (final concentration of 100 μM) and 10 mM HEPES (pH 7.4, 5 mM $MgCl_2$) at 37℃ for 30 min. The followed detection procedure was the same as shown in the aforementioned experiment for ALP detection.

Results and discussion

The synthesized g-C_3N_4 nanosheets were characterized by means of transmission electron microscopy (TEM), atomic force microscopy (AFM), X-ray diffraction (XRD) and Fourier transform infrared spectroscopy (FT-IR). The average diameter of g-C_3N_4 nanosheets was estimate to be 120 nm according to TEM image (Fig. 1A). The thickness of the nanosheets was ~1.25 nm (Fig. 1C), evidencing that the as-prepared g-C_3N_4 nanosheets comprised less than four layers. The g-C_3N_4 nanosheets solution was clear and very stable, no sediment was observed after the solution was stored for several months. Moreover, a positive zeta potential of 25.2 mV was observed for the nanosheets solution, indicating a positive charged surface for the nanosheets which helped to maintain their good dispersibility in water (Fig. 1B). XRD patterns revealed that there was a strong XRD peak centered at 27.7° (d = 0.325 nm) corresponds to the reflection of g-C_3N_4 (Fig. S1, ESI†).[40] FT-IR was further performed to explore the chemical composition of the g-C_3N_4 nanosheets and absorption peaks were assigned for accordingly vibration bonds (Fig. S2, ESI†).

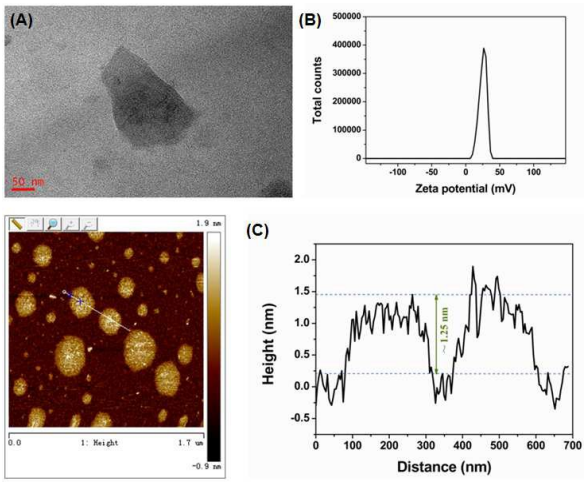

Fig. 1 (A) TEM image of the g-C_3N_4 nanosheets. (B) zeta potential of g-C_3N_4 nanosheets solution determined by DLS analysis. (C) AFM image of the g-C_3N_4 nanosheets (left) and the height profile of corresponding section (right).

Fig. 2 illustrates typical fluorescence responses of the g-C_3N_4 nanosheet based biosensor in the assays. The g-C_3N_4 nanosheets exhibits a strong fluorescence peak at 440 nm under excitation at 310 nm (plot a). The strong fluorescence of g-C_3N_4 nanosheets solution was observed to be substantially reduced upon the addition of Cu^{2+}, suggesting that Cu^{2+} could effectively quench the fluorescence of g-C_3N_4 nanosheets (plot b). The potential of the developed assay for ALP detection was demonstrated in plot c and d. Without introduction of ALP, incubation PPi with Cu^{2+} and g-C_3N_4 resulted in a strong fluorescence signal (plot c), corresponding to a fluorescence "turn on" state. This was ascribed to the chelation between PPi and Cu^{2+}, which prevented the coordination between Cu^{2+} and g-C_3N_4 nanosheets and inhibited the quenching effect induced by Cu^{2+}. In contrast, in the presence of ALP, much lower fluorescence was observed, corresponding to a fluorescence "turn off" state which was attributed to the ALP-catalyzed conversion of PPi into Pi with much weaker affinity to chelate with Cu^{2+} (plot d).

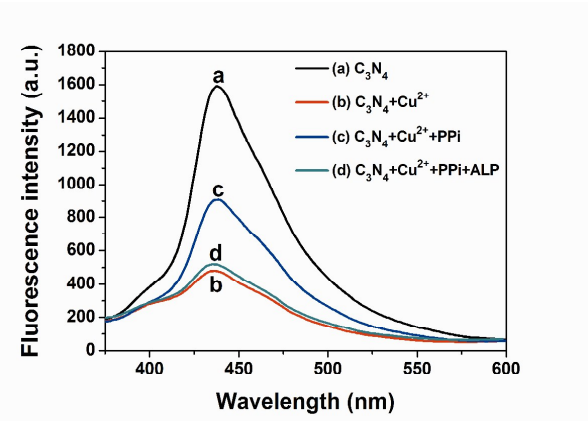

Fig. 2 Fluorescence emission spectra of (a) g-C_3N_4, (b) g-C_3N_4 + Cu^{2+}, (c) g-C_3N_4 + Cu^{2+} +PPi, and (d) g-C_3N_4 + Cu^{2+} +PPi + ALP . All the reactions were performed in 10 mM HEPES containing 5 mM $MgCl_2$ at pH 7.4. All of the g-C_3N_4 concentrations were 5 μg mL^{-1}; Cu^{2+} concentrations were 20 μM in (a), (b) and (c); PPi concentrations were 100 μM in (c) and (d); ALP concentration was 5000 U/L in (d). Excitation: 310 nm and emission: 440 nm.

To demonstrate mechanism of fluorescence quenching and restoring of the system, we performed fluorescence lifetime measurements for this system. The fluorescence decay curves (Figure S3, ESI) were fitted using a biexponential model and the lifetimes for all components were then calculated (Table S1, ESI). The fluorescence lifetime for g-C_3N_4 was found to be 13.22 ns (94.25%) and 3.30 ns (5.75%), and the lifetime showed little change after the nanosheets interacted with Cu^{2+}. This finding implied the formation of a non-fluorescentcomplex between the nanosheets and Cu^{2+}. Presumably, because the redox potential of Cu^{2+}/Cu^{+} lay between the conductance band and the valence band of g-C_3N_4,[22, 32] efficient PET might occur in this complex, leading to substantial quenching of the fluorescence for g-C_3N_4. After the reaction of PPi in the complex, there was also no remarkable change of the fluorescence lifetime. This result indicated the displacement of Cu^{2+} by PPi from the complex, which resulted in the restoration of fluorescence.

The experiment conditions have been optimized for the ALP detection including the amount of Cu^{2+}, amount of PPi, reaction temperature and reaction time. The fluorescent intensities of g-C_3N_4 decreased with the increasing amount of Cu^{2+}, and leveled off when the concentration reached 20 μM (Fig. S4, ESI†). Then different concentrations of PPi (0 μM-400 μM) were added and fluorescence responses were recorded (Fig. S5A, ESI†). A linear relationship (y=4.26x+411.43, R^2=0.995) was obtained between the fluorescence intensity and the concentration of PPi range from 0-100 μM (Fig. S5B, ESI†). So 100 μM PPi was chosen to

benefit quantitative ALP activity assay. The reaction temperature and time were also investigated, 30 min was time chosen for ALP to catalyze the hydrolysis of its substrate PPi was 30 min and another 30 min was chosen to allow complete reaction among Cu^{2+}, PPi and g-C_3N_4 nanosheet (Fig. S6, ESI†). Hence, 20 μM Cu^{2+}, 100 μM PPi, 30 min incubation time for ALP catalytic reaction and 30 min incubation time for reaction among Cu^{2+}, PPi and g-C_3N_4 nanosheet at 37℃ were chosen as the optimal conditions for ALP assay as described in the experimental section.

With the optimized conditions, the ability of the g-C_3N_4 nanosheet based biosensor for quantitative analysis of ALP was investigated by performing the assays with a series of different concentrations of ALP. As shown in Fig. 4, the fluorescence peak at 440 nm increases gradually with increasing concentrations of ALP range from 0.1 to 5000 U/L. A linear relationship (y=801.0-29.4x, R^2=0.993) was obtained between the fluorescence intensity and the concentration of ALP across a four-decade concentration range from 0.1 to 1000 U/L. The detection limit for ALP was estimated to be 0.08 U/L according to the 3σ rule. Such a low detection limit was significantly superior to or comparable with previous ALP assays (Table S2, ESI†). These results demonstrated that the developed approach held the potential as a highly sensitive platform for detecting ALP.

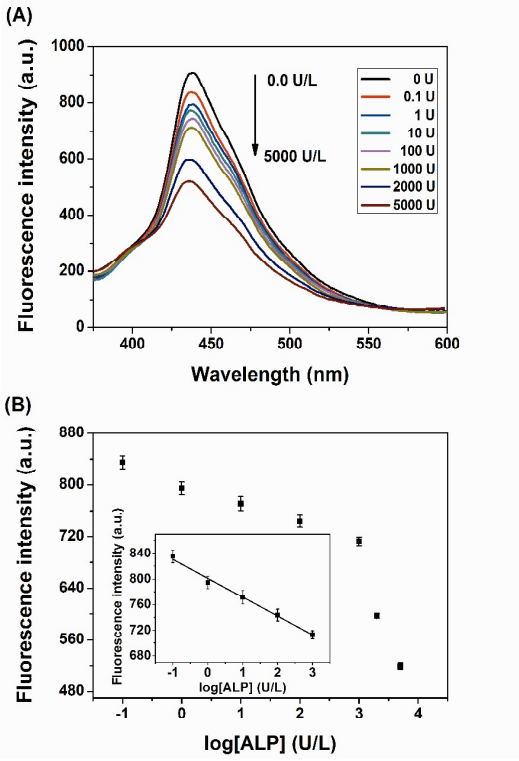

Fig. 3 (A) Fluorescence spectra of the developed assay in response to different concentrations of ALP. (B) The fluorescent intensity (at 440 nm) versus log value of ALP activity from 0 to 5000 U/L. inset: the linear fitting curve between fluorescence intensity and log value of ALP level from 0.1 to 1000 U/L. Excitation: 310 nm and emission: 440 nm.

To evaluate the selectivity of the developed assay, the fluorescent responses of other proteins possibly coexisting with ALP were detected. It was found that acetylcholinesterase (AChE), lysozyme, exo I, exo III, uricase and glucose oxidase showed no obvious fluorescence responses as measured using the proposed approach (Fig. 4). These results clearly demonstrated the method had desirable selectivity toward ALP.

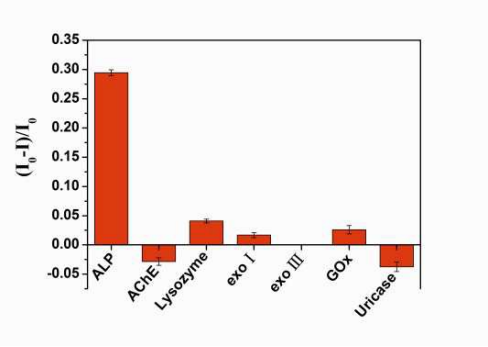

Fig. 4 The selectivity of the developed assay for ALP detection over other proteins. ALP was 1000 U/L (0.335 μM), AChE, lysozyme, exo I, exo III, GO_X and uricase were 0.68 μM.

Employing the proposed method, we were also able to screen potential inhibitors of ALP. The potassium phosphate monobasic, a known inhibitor of ALP, was tested to examine the ability of the developed assay for screening ALP inhibitors. It was observed that the activity of ALP decreased with increasing concentration of KH_2PO_4 (Fig. 5). These results suggested the potential use of the proposed method for studies of ALP inhibition and it could be extended to screen inhibitors of ALP.

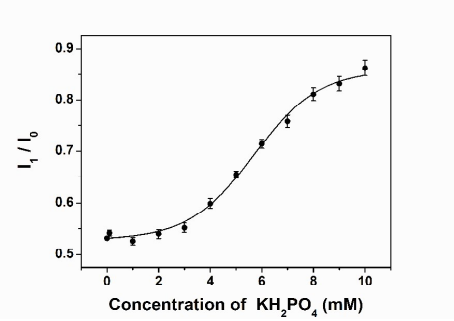

Fig. 5 Fluorescence responses of the developed assay for different concentrations of ALP inhibitor (KH_2PO_4).

To evaluate the applicability of the developed assay to complex biological media, the assay for ALP in diluted serum specimen was performed. Four serum samples with added ALP of different concentrations were measured using the developed method (Table S3, ESI). The results revealed that our method gave acceptable recoveries in the range from 91.5% to 101%, indicating the potential of the developed method for analysis of real biological samples.

Conclusions

In conclusion, we have developed a novel fluorescent g-C_3N_4 nanosheet based biosensor for highly sensitive, label-free detection of alkaline phosphatase (ALP). The proposed method is rapid, simple and implemented in a homogeneous format. Compared to existing methods for ALP assay typically involving the use of synthetic substrates, the developed approach utilizes a natural substrate of ALP in biological systems, which may afford higher catalytic efficiency toward this substrate and thus provide much better sensitivity for ALP detection. Relative to recently reported assays for ALP based on nobel metal nanoclusters, g-C_3N_4 shows higher luminenscent intensity as well as photo and chemical stability, which may ensure improved sensitivity and selectivity for the developed approach in ALP detection. The developed approach has been demonstrated to provide excellent selectivity and superior sensitivity compared with existing methods. Hence, the developed method may hold great potential for ALP-based clinical diagnostics and biomedical applications.

Acknowledgement

This work was supported by NSFC (21527810, 21190041, 21307029, 21221003) and National Key Basic Research Program (2011CB911000).

Notes and references

1 K. S. Novoselov, A. K. Geim, S. V. Morozov, D. Jiang, Y. Zhang, S. V. Dubonos, I. V. Grigorieva and A. A. Firsov, *Science*, 2004, **306**, 666–669.

2 D. Chen, H. B. Feng and J. H. Li, *Chem. Rev.*, 2012, **112**, 6027-6053.

3 A. A. Balandin, S. Ghosh, W. Z. Bao, I. Calizo, D. Teweldebrhan, F. Miao and C. N. Lau, *Nano Lett.*, 2008, **8**, 902–907.

4 C. H. Lu, H. H. Yang, C. L. Zhu, X. Chen and G. N. Chen, *Angew. Chem. Int. Ed.*, 2009, **48**, 4785–4787.

5 H. X. Chang, L. H. Tang, Y. Wang, J. H. Jiang and J. H. Li, *Anal. Chem.*, 2010, **82**, 2341–2346.

6 S. J. He, B. Song, D. Li, C. F. Zhu, W. P. Qi, Y. Q. Wen, L. H. Wang, S. P. Song, H. P. Fang and C. H. Fan, Adv. *Funct. Mater.*, 2010, **20**, 453–459.

7 M. Yi, S. Yang, Z. Y. Peng, C. H. Liu, J. S. Li, W. W. Zhong, R. H. Yang, and W. H. Tan, *Anal. Chem.*, 2014, **86**, 3548–3554.

8 C. H. Lu, C. L. Zhu, J. Li, J. J. Liu, X. Chen and H. H. Yang, *Chem. Commun.*, 2010, **46**, 3116–3118.

9 H. F. Zhao, R. P. Liang, J. W. Wang and J. D. Qiu, *Biosens. Bioelectron.*, 2015, **63**, 458–464.

10 J. Lee, G. Park and D. H. Min, *Chem. Commun.*, 2015, **51**, 1459–14600.

11 Z. H. Yang, Y. Zhuo, R. Yuan,Y. Q. Chai, *Biosens. Bioelectron.*, 2015, **69**, 321–327.

12 C. F. Zhu, Z. Y. Zeng, H. Li, F. Li, C. H. Fan and H. Zhang, *J. Am. Chem. Soc.*, 2013, **135**, 5998–6001.

13 Q. Xi, D. M. Zhou, Y. Y. Kan, J. Ge, Z. K. Wu, R. Q. Yu and J. H. Jiang, *Anal. Chem.*, 2014, **86**, 1361–1365.

14 R. L. Liu, D. Q. Wu, X. L. Feng and K. K. Müllen, *J. Am. Chem. Soc.*, 2011, **133**, 15221–15223.

15 G. Eda, Y. Y. Lin, C. Mattevi, H. Yamaguchi, H. A. Chen, I. S. Chen, C. W. Chen and M. Chhowalla, *Adv. Mater.*, 2010, **22**, 505–509.

16 E. L. K. Chng, Z. Sofer and M. Pumera, *Nanoscale*, 2014, **6**, 14412–14418.

17 Y. Wang, Y. Y. Shao, D. W. Matson, J. H. Li and Y. H. Lin, *ACS. Nano.*, 2010, **4**, 1790–1798.

18 X. D. Zhang, X. Xie, H. Wang, J. J. Zhang, B. C. Pan and Y. Xie, *J. Am. Chem. Soc.*, 2013, **135**, 18–21.

19 Q. J. Lu, J. H. Deng, Y. X. Hou, H. Y. Wang, H. T. Li and Y. Y. Zhang, *Chem. Commun.*, 2015, **51**, 12251–12253.

20 Q. B. Wang, W. Wang, J. P. Lei, N. Xu, F. L. Gao and H. X. Ju, *Anal. Chem.*, 2013, **85**, 12182–12188.

21 X. J. Liao, Q. B. Wang and H. X. Ju, *Chem. Commun.*, 2014, **50**, 13604–13607.

22 E. Z. Lee, Y. S. Jun, W. H. Hong, A. Thomas and M. M. Jin, *Angew. Chem. Int. Ed.*, 2010, **49**, 9706–9710.

23 H. Li, M. M. Yang, J. Liu, Y. L. Zhang, Y. M. Yang, H. Huang, Y. Liu and Z. H. Kang, *Nanoscale*, 2015, **7**, 12068–12075.

24 E. Z. Lee, S. U. Lee, N. S. Heo, G. D. Stucky, Y. S. Jun and W. H. Hong, *Chem. Commun.*, 2012, **48**, 3942–3944.

25 X. L. Zhang, C. Zheng, S. S. Guo, J. Li, H. H. Yang and G. N. Chen, *Anal. Chem.*, 2014, **86**, 3426–3434.

26 M. C. Rong, L. P. Lin, X. R. Song, T. T. Zhao, Y. X. Zhong, J. W. Yan, Y. R. Wang and X. Chen, *Anal. Chem.*, 2015, **87**, 1288–1296.

27 Y. R. Tang, H. J. Song, Y. Y. Su and Y. Lv, *Anal. Chem.*, 2013, **85**, 11876–11884.

28 Y. Kuang, J. F. Shi, J. Li, D. Yuan, K. A. Alberti, Q. B. Xu and Bing Xu, *Angew. Chem. Int. Ed.*, 2014, **53**, 8104–8107.

29 R. A. Pires, Y. M. Abul-Haija, D. S. Costa, R. Novoa-Carballal, R. L. Reis, R. V. Ulijn and I. Pashkuleva, *J. Am. Chem. Soc.*, 2015, **137**, 576–579.

30 Y. L. Xianyu, Z. Wang and X. Y. Jiang, *ACS Nano*, 2014, **8**, 12741–12747.

31 L. Y. Jin, Y. M. Dong, X. M. Wu, G. X. Cao and G. L. Wang, *Anal. Chem.*, 2015, **87**, 10429–10436.

32 J. Q. Tian, Q. Liu, A. M. Asiri, A. O. Al-Youbi and X. P. Sun, *Anal. Chem.*, 2013, **85**, 5595–5599.

33 L. L. Zhang, J. J. Zhao, M. Duan, H. Zhang, J. H. Jiang and R. Q. Yu , *Anal. Chem.*, 2013, **85**, 3797–3801.

34 J. J. Deng, P. Yu, L. F. Yang and L. Q. Mao, *Anal. Chem.*, 2013, **85**, 2516–2522.

35 K. F. Xu, Z. H. Chen, L. Zhou, O. Zhen, X. P. Wu, L. H. Guo, B. Qiu, Z. Y. Lin and G. N. Chen, *Anal. Chem.*, 2015, **87**, 816–820.

36 L. Dong, Q. Q. Miao, Z. J. Hai, Y. Yuan and G. L. Liang, *Anal. Chem.*, 2015, **87**, 6475–6478.

37 J. J. Deng, P. Yu, Y. X. Wang and L. Q. Mao, *Anal. Chem.*, 2015, **87**, 3080–3086.

38 Y. Chen, H. P. Zhou, Y. Wang, W. Y. Li, J. Chen, Q. Lin and C. Yu, *Chem. Commun.*, 2013, **49**, 9821–9823.

39 X. Q. Liu, F. Wang, A. Niazov-Elkan, W. W. Guo and I. Willner. *Nano Lett.*, 2013, **13**, 309–314.

40 X. Wang, K. Maeda, A. Thomas, K. Takanabe, G. Xin, J. M. Carlsson, K. Domen and M. Antonietti, *Nat. Mater.*, 2009, **8**,76–80.

41 L. C. Chen, D. J. Huang, S. Y. Ren, T. Q. Dong, Y. W. Chi and G. N. Chen, *Nanoscale*, 2013, **5**, 225–230.

42 X. Wang, K. Maeda, X. Chen, K. Takanabe, K. Domen, Y. D. Hou, X.Z. Fu, M. Antonietti, *J. Am. Chem. Soc.*, 2009, **131**,1680–1681.